

RESEARCH

Open Access



Compatible traits of oleaginous Mucoromycota fungi for lignocellulose-based simultaneous saccharification and fermentation

Cristian Bolaño Losada^{1*}, Ondrej Slaný¹, Dana Byrtusová¹, Boris Zimmermann¹, Svein Jarle Horn², Achim Kohler¹ and Volha Shapaval¹

Abstract

Background Mucoromycota fungi are promising for the production of second-generation biofuel from single-cell oils (SCOs) using lignocellulose biomass. Despite the lack of enzymatic capability for efficiently degrading lignocellulose in Mucoromycota fungi, simultaneous saccharification and fermentation (SSF) offers an attractive solution by combining enzymatic hydrolysis and fermentation in the same procedure. This study explored specific traits of various Mucoromycota species to evaluate their suitability for SSF, due to the frequent and significant gap between the microorganism and enzyme optimal conditions.

Results The suitability of nine oleaginous fungal strains from the Mucoromycota phylum for use in lignocellulose-based simultaneous saccharification and fermentation was evaluated. Several traits, such as thermal tolerance, biochemical composition changes in response to incubation temperature, cellobiose and cellulose response and induction of β -glucosidase and endoglucanase, were evaluated. *Lichtheimia corymbifera* was the most suitable species for SSF due to its ability to grow up to 45 °C, with a consequent decrease in lipid unsaturation, and good uptake of cellobiose with induction of β -glucosidase and endoglucanase expression. The *Cunninghamella blackesleeana* and *Mucor circinelloides* strains were also considered good candidates; despite the cultivation should not exceed 35 °C, their good uptake of cellobiose and the expression of extracellular β -glucosidase induced by cellobiose indicated that they could increase the enzymatic hydrolysis efficiency. *C. blackesleeana* outperformed all the other tested strains in terms of β -glucosidase activity expression. In addition, both endoglucanase and β -glucosidase activities of *Rhizopus stolonifer* and *M. circinelloides* were induced by cellobiose. *Mortierella alpina* and *Mortierella hyalina* were not considered suitable for simultaneous saccharification and fermentation due to their reduced tolerance to high temperatures and poor response to cellobiose utilization.

Conclusions This study identified beneficial traits of Mucoromycota species for simultaneous saccharification and fermentation using lignocellulose, contributing to an optimal selection for producing lipid-derived second-generation biofuels.

Keywords Mucoromycota, Simultaneous saccharification and fermentation, Single-cell oils, Lignocellulose, Biofuels, Vibrational spectroscopy, Thermal tolerance, Cellulases

*Correspondence:

Cristian Bolaño Losada

cristian.bolano.losada@nmbu.no

Full list of author information is available at the end of the article



© The Author(s) 2025. **Open Access** This article is licensed under a Creative Commons Attribution-NonCommercial-NoDerivatives 4.0 International License, which permits any non-commercial use, sharing, distribution and reproduction in any medium or format, as long as you give appropriate credit to the original author(s) and the source, provide a link to the Creative Commons licence, and indicate if you modified the licensed material. You do not have permission under this licence to share adapted material derived from this article or parts of it. The images or other third party material in this article are included in the article's Creative Commons licence, unless indicated otherwise in a credit line to the material. If material is not included in the article's Creative Commons licence and your intended use is not permitted by statutory regulation or exceeds the permitted use, you will need to obtain permission directly from the copyright holder. To view a copy of this licence, visit <http://creativecommons.org/licenses/by-nc-nd/4.0/>.

Background

Single-cell oils (SCOs) are lipids accumulated intracellularly in oleaginous organisms, mostly in the form of triacylglycerols (TGAs). Oleaginous organisms are defined as microorganisms that can accumulate lipids intracellularly, comprising more than 20% of their dry weight [1], with some of them capable of accumulating up to the astounding amount of 80%_{w/w} [2]. The ability to be oleaginous has been observed in different microorganisms, such as bacteria [3], algae [4], yeasts [5], thraustochytrids [6], and filamentous fungi [7–9]. In general, the most effective way to trigger lipogenesis in oleaginous microorganisms is to use a cultivation medium with a high carbon-to-nitrogen ratio [10]. Oleagenicity is especially common in fungi from the phylum Mucoromycota [11, 12]. Several Mucoromycota species have already been used for single-cell oil (SCO) production at industrial scale, such as the production of gamma-linolenic acid by *Mucor circinelloides* by John & E. Sturge Ltd. (United Kingdom), which has not succeeded on the market due to the low prices of alternative vegetable oils [13], or the production of arachidonic acid using *Mortierella alpina* by DSM (The Netherlands), with increasing market demand [14].

In general, SCO biorefineries based on filamentous fungi are still uncommon since their economic viability depends on the selection of the right microbial producer, feedstock, ability to coproduce other valuable products, process configuration, lipid recovery method, etc. [9]. Taking these considerations into account, Mucoromycota fungi have several advantages for SCO biorefineries: (1) generally faster growth than Ascomycota and Basidiomycota [15]; (2) the ability to utilize a plethora of substrates, either refined or low-cost ones; and (3) the ability to coproduce other valuable compounds, including carotenes, organic acids, and amino polysaccharides, such as chitin and chitosan [16]. Moreover, Mucoromycota fungi can adapt to many fermentation process configurations, such as classical submerged fermentation [17] or solid-state fermentation [18].

In the context of potential new biorefineries, simultaneous saccharification and fermentation (SSF) is a relevant fermentation process for the valorization of lignocellulosic feedstocks. SSF is a process in which enzymatic hydrolysis of lignocellulose substrates and growth of a microorganism of interest occur at the same time, simplifying the whole process and reducing costs compared to separate hydrolysis and fermentation [19]. When lignocellulosic materials are used as feedstocks for biofuel production, i.e., bioethanol or lipids for biodiesel, they are classified as second-generation biofuels. SSF has emerged as a relevant process to fit the actual regulation's requirements for second-generation biofuels at a reduced

cost of production. Although lignocellulose-based SSF has been reported for a few species of Mucoromycota, such as *Mucor indicus* and *Rhizopus oryzae* for ethanol production [20], according to the author's knowledge, the suitability of oleaginous Mucoromycota for lipid production using SSF has not been reported in the literature.

Cellulytic enzymes are crucial components of SSF in terms of hydrolysis efficiency and operational cost. Regarding the hydrolysis efficiency, a general disadvantage is the gap between the optimal conditions for cellulase activity (50 °C and pH 4.5–5.5) and the optimal conditions for the growth of microorganisms (25–30 °C, pH 6.0–7.0) [21]. Hence, a compromise between these two sets of conditions needs to be found. Notably, the benefits become more evident when the optimal temperature of a microorganism aligns well with the optimal temperature for enzyme activity. In terms of costs, the use of commercial enzymes can account for 28% of the operational costs of SSF for ethanol production [22]. Several techno-economical studies suggest that a viable strategy for reducing costs is to design a process that includes on-site cellulase production, thereby preventing the purchase of expensive commercial enzymes [19, 23]. This alternative is attractive since the costs associated with long-term storage, use of additives, and transportation are avoided. Consequently, this approach can result in a 30–70% reduction in enzyme-related costs. For instance, this strategy was followed by Clariant AG (Switzerland) in its Sunliquid® process to produce bioethanol from wheat straw [24]. Unfortunately, this process was discontinued in 2023, it is common that lignocellulosic ethanol plants struggle to be economically viable due to the production cost and market prices, although this can change with future biofuel regulations [25]. The most common organism used for cellulase production is *Trichoderma reesei*, which has been studied for more than 70 years, is used for industrial-scale cellulase production [26], and is also frequently recommended for on-site cellulase production [27, 28]. However, one drawback of this fungus is that a major part of the β -glucosidase remains bound to the cell wall making its recovery difficult [29]. β -glucosidase is considered a bottleneck in the overall reaction of cellulose hydrolysis since the accumulation of its substrate, cellobiose, promotes the inhibition of endoglucanase and cellobiohydrolase [30]. This problem can be solved by supplementing β -glucosidase separately produced from another microorganism, which might not be preferable for on-site production. Genetic manipulation through random or direct mutagenesis is another possibility to overcome these challenges. While the organisms obtained by random mutagenesis are not classified as genetically modified organisms (GMO), direct mutagenesis requires significant investments in

research and development (R&D), approval of GMO use and regulations, implementation of containment measurements, testing, and scale-up, etc. Thus, the use of a hypersecreting *Trichoderma reesei* obtained by random mutagenesis, such as the commercially available strain RUT C-30, might be a preferable cost-effective short-term option for the bioprocess development despite of still face the aforementioned challenges at some degree. Therefore, when β -glucosidase activity is deficient, selecting a microorganism for SSF that can directly utilize cellobiose, either by uptake or by extracellular expression of β -glucosidase is desirable. Additionally, it is also desirable if cellobiose can trigger the expression of other cellulases such as endoglucanase.

Mucoromycota fungi do not have complete cellulase enzyme systems; for example, they lack cellobiohydrolases, which hinders their efficiency in cellulose degradation [31, 32]. However, they can produce β -glucosidase and endoglucanase [33–35]. The production of β -glucosidase improves the enzymatic hydrolysis efficiency by processing cellobiose and thus alleviating enzyme inhibition. The importance of this capability is underscored by numerous studies on improving the efficiency of ethanol production by yeast in SSF, either by performing genetic modifications of species that lack cellodextrin processing tools [36–41] or by finding species that can grow on cellobiose [42]. Notably, high glucose concentrations also result in feedback inhibition of β -glucosidase. However, the presence of the microorganism in SSF leads to an immediate removal of glucose as it is generated, thus mitigating the inhibitory effect [43].

In the present study, the suitability of oleaginous Mucoromycota for SSF was assessed for a diverse set of strains, which have been extensively studied in previous research [2, 44, 45]. The main aim of this study was to determine relevant traits for SSF in this set of strains, namely,

thermal tolerance, and cellulase expression in the presence of cellobiose and cellulose. In addition to growth rates, enzyme expression, and specific activities; vibrational spectroscopy techniques (FTIR and FT-Raman) were also used to evaluate the effect of the incubation temperature on the fungal biomass composition. These techniques have been proven to be reliable and reproducible methods for characterizing fungal biomass [11, 46, 47].

Materials and methods

Fungal strains

Nine strains belonging to eight different species of Mucoromycota fungi were used in this study. The strains were obtained from the Czech Collection of Microorganisms (CCM; Brno, Czech Republic), the Norwegian School of Veterinary Science (VI; Ås, Norway), the All-Russian Collection (VKM, Pushchino, Russia), and the American Type Culture Collection (ATCC; Manassas, United States). The list of strains and motivations for their selection are summarized in Table 1.

Spore and stock culture preparations

All the fungal strains were stored in the form of spore solutions in 33%_{v/v} glycerol at $-80\text{ }^{\circ}\text{C}$, except for *Mortierella alpina*, which was subcultured regularly by transferring agar plugs with mycelia to a new fresh medium. Malt extract agar (MEA) (Merck, Germany), composed of agar, 15 g/L; malt extract, 30 g/L; mycological peptone, 5 g/L, and pH 5.4, was used as the medium for preparation of the stock cultures. MEA plates were prepared by dissolving 50 g of MEA powder in 1 L of distilled water and autoclaving at $121\text{ }^{\circ}\text{C}$ for 15 min. All the strains were cultivated at $25\text{ }^{\circ}\text{C}$ for 7–14 days until spores were obtained. The fresh spores were collected by adding

Table 1 List of fungal strains and motivations for their selection

Species	Collection number	Abbreviation	Motivation
<i>Lichtheimia corymbifera</i>	CCM 8077	LC	Fatty acid profile with good cetane number for biodiesel production [11]
<i>Absidia glauca</i>	CCM F451	AG	High lipid content [11], and coproduction of chitosan [48]
<i>Cunninghamella blakesleeana</i>	CCM F705	CB	Fatty acid profile with good cetane number for biodiesel production [44]
<i>Mortierella alpina</i>	ATCC 32222	MA	Relevant for arachidonic acid production at industrial scale [14] and other polyunsaturated fatty acids (PUFAs)
<i>Mucor circinelloides</i>	CCM F220	MC	Model species for lipogenesis studies and dimorphism [49]. First species with annotated genome among Mucoromycota. Industrially relevant for gamma-linolenic acid production [13]. Coproduction of high-value metabolites [2, 45, 50]
<i>Mucor circinelloides</i>	VI04473	MCVI	
<i>Mortierella hyalina</i>	VKM F1629	MH	Promising producer of arachidonic acid and other PUFAs [11]
<i>Rhizopus stolonifer</i>	VKM F400	RS	High linolenic acid accumulation [11] and industrially relevant genus for fumaric and lactic acid production [51]
<i>Umbelopsis vinacea</i>	CCM F539	UV	Fatty acid profile with good cetane number for biodiesel production [11]

10 mL of sterile 0.9% NaCl solution and dragging the mycelium with a glass Digralsky spreader.

Thermal tolerance range

The thermal tolerance range of the strains was determined by measuring the growth of the colony diameter in agar medium at different temperatures following the procedure of Trinci with some modifications [52]. MEA was used as medium, dispensing a volume of 20 mL into each tripled-vented Petri dish to avoid any variability related to volume differences. A preinoculum of mycelium for each strain was prepared by plating 10 μ L of spore stock in the center of the MEA plate. The preinoculum plates were cultivated at 25 °C until a large colony was obtained with active growing mycelium at the edge. A cork borer no. 2 was used to cut circular agar plugs with active growing mycelium. The agar plugs were placed on the center of the 20 mL MEA plates for the thermal tolerance range test. The MEA plates were incubated at a selected range of temperatures (20, 25, 30, 35, 40, 45, and 50 °C). The experiment was performed in triplicate for each temperature and strain. The extension of the colony was determined by taking two measurements of the colony diameter, orthogonal to each other, at least twice per day until the colony covered the whole area of the plate. The growth rate (K_r ; colony diameter mm/hour) was obtained from the slope of the linear equation fitted to the average diameter values versus the incubation time.

After a total extension of the colony was achieved, the spores were washed away with sterile 0.9% NaCl solution several times until the washing solution was free of spores. The spore-free mycelium was removed from the agar medium with the help of a scalpel without removing the agar. The mycelium was further washed to remove possible soluble compounds by adding 10 mL of 0.9% NaCl solution, centrifuging, and discarding the supernatant a total of three times. The mycelium was frozen at -20 °C and freeze-dried until constant dry weight. The dried samples were stored at -20 °C until further analysis.

Cellulase induction by the presence of cellobiose and cellulose

The spores for inoculation of the experiments described in this section were obtained as previously described. The suspension of spores from the MEA plates was clarified through two-layer sterile Miracloth 22–25 μ m pore size (Merck, Germany) and counted using an automated cell counter (Countess 3; Invitrogen, United States).

To evaluate how the different *Mucoromycota* strains respond to the presence of cellobiose, a cellobiose-based medium was prepared with carbon and nitrogen components as described by Takó et al. [33] and with macro- and

micronutrients as described by Kosa et al. [44] (g/L): cellobiose, 10; yeast extract, 0.5; $(\text{NH}_4)_2\text{SO}_4$, 1.5; sodium glutamate, 1.5; Na_2HPO_4 , 2; KH_2PO_4 , 7; $\text{MgSO}_4 \cdot 7\text{H}_2\text{O}$, 1.5; $\text{CaCl}_2 \cdot 2\text{H}_2\text{O}$, 0.1; $\text{FeCl}_3 \cdot 6\text{H}_2\text{O}$, 0.008; $\text{ZnSO}_4 \cdot 7\text{H}_2\text{O}$, 0.001; $\text{CuSO}_4 \cdot 5\text{H}_2\text{O}$, 0.0001; $\text{Co}(\text{NO}_3)_2 \cdot \text{H}_2\text{O}$, 0.0001; $\text{MnSO}_4 \cdot 5\text{H}_2\text{O}$, 0.0001, and pH 6.5. The cultivations were performed using a Duetz microtiter plate system (MTPS) consisting of 24 extra high deep well microtiter plates (EnzyScreen, The Netherlands, Cat #CR1424hd), low evaporation sandwich covers, and a clamp system for the shaker incubator. A volume of 5.6 mL of 1.25-fold medium was dispensed in each well, and 1.4 mL of prepared spore solution was added to provide an inoculum of 1.10^5 spores/mL. Each strain was grown in triplicate for each time point, meaning 2, 4, 6, and 8 days. The plates were incubated at 25 °C and 400 rpm in a MaxQ™ 4000 shaker (Thermo Scientific, United States). After the incubation, each sample was collected in a pre-weighed 15-mL Falcon tube and spun at 10,000 rpm in a Hermle Z326K centrifuge (Hermle, Germany), after which the supernatant was saved in a separate tube. The biomass was washed with distilled water, centrifuged at 10000 rpm 10 min and 4 °C, and the supernatant was discarded, repeating these steps three times. The washed biomass was freeze-dried until constant weight to determine the dry weight. The supernatant and the freeze-dried biomass samples were stored at -20 °C until further analysis.

To evaluate how the different strains respond to the presence of cellulose, a two-step cultivation was performed using the aforementioned Duetz-MTPS system. In the first cultivation step, 7 mL of potato dextrose broth (PDB) was inoculated with spores (1.10^5 spores/mL) and incubated for 3 days at 25 °C and 400 rpm. The inoculum for the *M. alpina* strain consisted of a homogenate of four agar plugs with active mycelium cut with a cork borer no. 5 (10 mm \varnothing) in 10 mL of 0.1% NaCl sterile solution. In the second cultivation step, the pregrown biomass was washed from PDB three times with 0.9% NaCl and centrifugation as previously described. Afterwards, 7 mL of cellulose-based medium was added, and the mixture was incubated for 4 days at 25 °C and 400 rpm. The PDB medium (glucose 20 g/L; potato infusion 4 g/L; Merck, Germany) was prepared by dissolving 24 g in 1 L of distilled water and autoclaved at 121 °C for 15 min. The cellulose-based medium consisted of (g/L) Avicel PH101 (microcrystalline cellulose powder), 20; NaNO_3 , 3; Na_2HPO_4 , 2; KH_2PO_4 , 7; $\text{MgSO}_4 \cdot 7\text{H}_2\text{O}$, 1.5; $\text{CaCl}_2 \cdot 2\text{H}_2\text{O}$, 0.1; $\text{FeCl}_3 \cdot 6\text{H}_2\text{O}$, 0.008; $\text{ZnSO}_4 \cdot 7\text{H}_2\text{O}$, 0.001; $\text{CuSO}_4 \cdot 5\text{H}_2\text{O}$, 0.0001; $\text{Co}(\text{NO}_3)_2 \cdot \text{H}_2\text{O}$, 0.0001; $\text{MnSO}_4 \cdot 5\text{H}_2\text{O}$, 0.0001; and pH 6.5. The experiment was performed in triplicate. At the end of the cultivation, the samples were collected, and the pellet and supernatant

were separated, processed, and stored in the same way as described previously.

The pH of the supernatants was measured using an Education Line EL2 pH meter (Mettler Toledo, Switzerland). The soluble protein concentration was determined by a 96-well plate Bradford method according to Ernst & Zor [53]: (1) bovine serum albumin (BSA) was used as standard; (2) 100 μL of the standard solution or sample was mixed with 100 μL of 2.5 diluted in water solution from concentrated Bradford reagent (Bio-Rad, United States, Cat #5,000,006); (3) 200 μL of distilled water was used as a blank; (4) the reaction mixtures were kept at room temperature for 10 min; and (5) the absorbance was measured at 590 nm and 450 nm (to use as ratio 590 nm/450 nm) with a UV/Vis spectrophotometer SPECTROstar Nano (BMG Labtech, Germany). The β -glucosidase activity was determined in 96-well plates following the method of Sonia et al. [54] with some modifications: (1) *p*-nitrophenol solution in sodium citrate buffer (50 mM, pH 4.8) was used as standard; (2) the reaction mixture consisted of 25 μL of supernatant or standard solution, 50 μL of sodium citrate buffer (50 mM pH 4.8) and 25 μL of *p*-nitrophenyl- β -D-glucopyranoside (*p*-NPG) 10 mM solution; (3) the plate was closed with a plastic plate seal to avoid evaporation, and the reaction was incubated at 50 °C for 30 min in darkness; (4) immediately after the incubation, 100 μL of NaOH-glycine buffer (400 mM, pH 10.8) were added to stop the reaction and increase the absorbance of the cleaved *p*-nitrophenol; and (5) the absorbance is measured at 405 nm. Endoglucanase activity was determined by the carboxymethylcellulose (CMC) and 3,5-dinitrosalicylic acid (DNS) method following the protocol of Samira et al. [55] with some modifications: (1) glucose is used as standard solution; (2) the reaction mix consisting of 100 μL sample or standard and 100 μL of 2%_{w/v} CMC solution in sodium citrate buffer (50 mM, pH 4.8) was incubated at 50 °C for 60 min; (3) after the reaction, 1 mL of DNS reagent was added, boiled at 95 °C for 10 min, and cold down on ice; (4) the absorbance at 540 nm is measured in semi-macro cuvettes of 1 cm pathlength. One enzymatic unit (U) was defined as the amount of enzyme needed to catalyze 1 μmol of substrate per minute. The specific enzymatic activity was calculated by dividing the total enzymatic activity by the amount of extracellular protein to account for the enrichment of a particular enzyme activity in the total protein mixture.

Sample processing for FTIR and Raman measurements

The freeze-dried samples from the thermal tolerance range assay were processed for FTIR and Raman measurements. For FTIR analysis, 3–5 mg of freeze-dried biomass was added to 2 mL polypropylene disruptor tubes

with 250 mg of acid-washed beads of 710–1180 μm diameter (Merck, Germany) and 400–500 μL of distilled water. The samples were disrupted by bead beating using a Precellys Evolution tissue homogenizer (Bertin Technologies, France) with the following settings: 5500 rpm and 20 s for 6 cycles. For FT-Raman analysis, the freeze-dried biomass was placed in a 400- μL flat bottom glass insert vial (Agilent Technologies, United States).

FTIR spectroscopy measurements

The FTIR spectra were recorded using a high-throughput screening module (HTS-XT) coupled to a Vertex70-FTIR spectrometer (both Bruker Optik GmbH, Germany) equipped with a globar mid-IR source and a deuterated L-alanine doped triglycine sulphate (DLaTGS) detector. 8 μL of disrupted and homogenized biomass was spotted onto an IR-transparent 384-well silicon microplate (Bruker Optik GmbH, Germany) and dried at room temperature, after which the microplate was placed in an HTS-XT module. Spectra were acquired in transmission mode, with a total of 64 scans, spectral resolution of 6 cm^{-1} , digital spacing of 1.928 cm^{-1} , over the range of 4000 to 400 cm^{-1} , using Blackman–Harris 3-term apodization, and an aperture of 6 mm. Spectra were recorded as the ratio of the sample spectrum to the spectrum of the empty IR-transparent microplate. Each biomass sample was analyzed in three technical replicates, resulting in 288 spectra. The OPUS software (Bruker Optik GmbH, Ettlingen, Germany) was used for data acquisition and instrument control.

FT-Raman spectroscopy measurements

The FT-Raman spectra were recorded using a MultiRAM FT-Raman spectrometer (Bruker Optik GmbH, Germany) equipped with a neodymium-doped yttrium aluminum garnet (Nd:YAG) laser (1064 nm, 9394 cm^{-1}) and a germanium detector cooled with liquid nitrogen, by using a high-throughput setup with 2.5 mm aperture and a collecting mirror objective. Approximately 10–20 mg of freeze-dried biomass was placed in a 400 μL flat-bottom glass insert vial, the sample vials were placed in a 96-well microplate, the microplate was placed in a high-throughput screening (HTS) stage, and the laser was focused on the bottom of the vial. The FT-Raman spectra were acquired in backscattering geometry with a total of 2048 scans, using Norton–Beer medium apodization, spectral resolution of 8 cm^{-1} , and digital spacing of 1.928 cm^{-1} , over the range 3785–45 cm^{-1} , at 500 mW laser power. For each biomass sample, at least one Raman spectrum was acquired, except both *Mucor circinelloides* strains samples, from which two or more technical replicates were measured for 25 °C, 30 °C, and 35 °C, resulting in 109 spectra. Due to the dark coloration derived from

sporangium, some samples were burnt, and the acquisition was not possible for all the *Absidia glauca* samples except one biological replicate at 20 °C; one biological replicate at 25 °C from *M. circinelloides* VI, *Rhizopus stolonifer*, and *Umbelopsis vinacea*; and one biological replicate at 20 °C from *M. circinelloides*. The OPUS software (Bruker Optik GmbH, Ettlingen, Germany) was used for data acquisition and instrument control.

Spectral preprocessing and data analysis

The FTIR spectra for principal component analysis (PCA) were preprocessed as follows: (1) smoothing with Savitzky–Golay algorithm (polynomial order 2, window size 11); (2) extended multiplicative signal correction (EMSC) (MSC model extended by a linear and quadratic components with polynomial order 2) [56]; and (3) data truncation from 700 to 3200 cm^{-1} .

To study the effect of cultivation temperature on lipid accumulation and unsaturation, the FTIR spectra were preprocessed with Savitzky–Golay algorithm with polynomial order 2, window size of 11, and second derivative. The ratio between the peaks at 3010 cm^{-1} (related to =CH stretching in aliphatics) and 2925 cm^{-1} (related to -CH stretching in -CH₂ group) was used as an indicator of unsaturation, while the ratio between 1745 cm^{-1} (C=O stretching related to triacylglycerol's bond) and 1650 cm^{-1} (amide I band) was used as lipid-to-protein ratio.

The FT-Raman spectra were preprocessed as follows: (1) smoothing by Savitzky–Golay algorithm with polynomial order 2, window size of 15, and derivative order 2 [57], (2) truncation of data from 900 to 1900 cm^{-1} , and (3) vector normalization. Averaged spectra were used for graphical visualization.

Biochemical similarities between samples were estimated by using principal component analysis (PCA). PCA was conducted on 288 FTIR spectral data. All the preprocessing, spectral visualization, and PCA were performed using Orange Data Mining version 3.33.0 (University of Ljubljana, Slovenia) [58, 59]. Biomass concentrations, growth rates, β -glucosidase activity, endoglucanase activity, extracellular protein concentrations, lipid-to-protein ratios, unsaturation ratios, and pH were analyzed and visualized using Excel.

Results and discussion

Thermal tolerance range

The Mucoromycota strains used in this study exhibited diverse growth rates at different temperatures when grown on MEA (Fig. 1). In ascending order, the optimal temperature for the growth of the strains was 20 °C for *Absidia glauca* (AG) and *Mortierella hyalina* (MH); 25 °C for *Mortierella alpina* (MA) and *Rhizopus stolonifer*

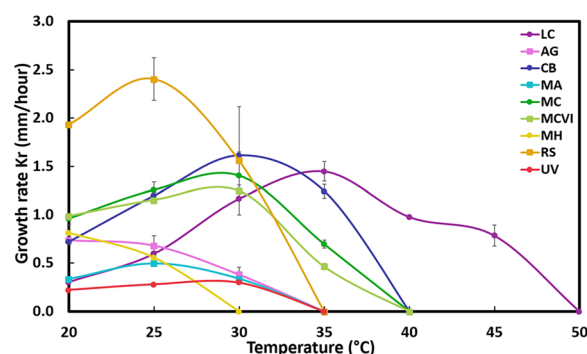


Fig. 1 Growth rates of nine Mucoromycota strains incubated at 20, 25, 30, 35, 40, 45 and 50 °C. Error bars represent the standard deviation of three biologically independent replicates

(RS); 30 °C for *Umbelopsis vinacea* (UV), *Cunninghamella blakesleeana* (CB), and the two strains of *Mucor circinelloides* (MCV and MC); and 35 °C for *Lichtheimia corymbifera* (LC). *L. corymbifera* displayed the widest range of growth supporting temperatures from 20 °C to 45–50 °C, in contrast to *M. hyalina*, whose growth was limited to below 30 °C. The strains *C. blakesleeana*, *M. circinelloides*, and *M. circinelloides* VI grew well at temperatures close to 35–40 °C, while *R. stolonifer*, *A. glauca*, *M. alpina*, and *U. vinacea* had shorter temperature tolerance range, with a maximum temperature ranging from 30–35 °C. With respect to the magnitude of the growth rate, *R. stolonifer* displayed the highest value of 2.4 mm/h at 25 °C among all the strains tested. The fast propagation of *R. stolonifer* provides an advantage for the colonization and infection of vegetables, fruits, and food, which is a characteristic of this species [60].

In terms of suitability for SSF, among the studied Mucoromycota strains, *L. corymbifera* is the strain that best aligns with the optimal temperature for enzymatic hydrolysis (50 °C). *L. corymbifera* is a known thermotolerant species, with some strains even able to grow at 50 °C [61]. However, for the strain studied in this work, the temperature should be restricted to 40–45 °C. However, despite the optimal activity of cellulases being found at 50 °C, the thermal deactivation of the enzymes is lower at 40 °C, and since fungal fermentation often takes 72 h or longer, the final hydrolysis yield can be superior because the enzymes remain active for a longer time [62]. On the other hand, *C. blakesleeana*, *M. circinelloides*, and *M. circinelloides* VI could also be suitable for the SSF process with cultivation temperatures around 35–37 °C. These temperatures are, in fact, typical in SSF for ethanol production with yeasts [43]. However, *A. glauca*, *M. alpina*, and *U. vinacea* can be cultivated only at 30 °C and *M. hyalina* at 25 °C, which makes them impractical for SSF. For these strains, other strategies could be applied,

such as a short prehydrolysis period at the optimal temperature of cellulases followed by inoculation and fermentation at a lower optimal growth temperature.

Effect of temperature on the fungal biomass composition

The composition of the fungal biomass from the thermal tolerance range experiment was analyzed by FTIR and Raman spectroscopy. High temperature is ideal for SSF, but high temperature may affect the quality and composition of the target product of fermentation, which in the case of this study was the total lipid content and the fatty acid profile. Both FTIR and Raman spectroscopy are convenient methods to study lipid accumulation and fatty acid profile, especially when relatively small quantities of biomass are available, which limits the application of conventional techniques such as gas chromatography [46].

FTIR spectra were collected from all the samples, and PCA was performed to visualize the main biochemical differences between all the strains and among the temperature conditions (Fig. 2A). The whole spectra of each strain at different temperatures and several additional PCA for more detailed visualization can be found in the supplementary information (Fig. 1S and 2S). The principal components (PC), PC1 and PC2, gathered 67.1% and 14.7% of total explained variance. According to the loading plots (Fig. 2B), PC1 correlated positively with lipids, as indicated by the high positive loading values at 3010, 2925, and 2855 (=C-H stretching, -C-H stretching from -CH₃; -C-H stretching from -CH₂, respectively) 1745 (C=O stretching from esters), 1465 (C-H deformation from -CH₃ and -CH₂) and 725 cm⁻¹ (-CH₂ rocking in aliphatics); and negatively with polysaccharides indicated by negative loading values in the range of 1125–985 cm⁻¹ (C–O–C and C–O stretching). PC2 correlated positively with proteins with positive loadings associated with the amide bands at 1680–1630 (amide I), 1530–1560 (amide II and C–NH deformation), and 1325 cm⁻¹ (amide III) and negatively with lipids with negative loadings at 3010, 2925, 2855, 1745, 1462, and 723 cm⁻¹, as well as with the polysaccharide-related signals from 1200 to 985 cm⁻¹.

The PCA results showed that *Mortierella* species (MH and MA) had very different biomass compositions compared to those of the other strains. Despite their slow growth rates, the accumulation of lipids in *Mortierella* seemed to be better than the other studied strains. One possible reason could be the weak sporulation in *Mortierella* spp., since nutrients and energy are not diverted to sporulation and are invested in the accumulation of lipids on the vegetative hyphae. Overall, the *M. alpina*, *M. hyalina*, *U. vinacea*, and *C. blakesleeana* strains produced lower amounts of spores on MEA than the other strains (Fig. 3S). It is possible that the level of sporulation of each strain could influence the differences observed in

lipid accumulation. For instance, solid-state fermentation of *Cunninghamella* and *Mortierella* species has been reported to have better lipid production than *M. circinelloides* [63]. In addition, one recent study reported that an oleaginous *M. circinelloides* strain cultivated on high C/N agar medium produced more biomass from spores than from mycelia [64] and worse lipid accumulation than when the same strain was grown in practically the same medium but using submerged fermentation [65].

On the other hand, some correlations of biochemical composition with the temperature of incubation were observed. *R. stolonifer*, increased the amount of proteins with the increase of temperature from 20 to 30 °C, shown by the displacement of the samples in the positive direction in PC1 and PC2. The opposite was detected for *A. glauca* and *C. blakesleeana*, whose composition increased in polysaccharides to the detriment of proteins from 20 to 30 °C, shown by a displacement in the negative direction of PC1 and PC2. The *M. circinelloides* VI strain showed a trend in temperatures from 20 to 35 °C correlated positively with PC1 and negatively with PC2, which translated into an increase in lipid accumulation, whereas the *M. circinelloides* MC strain showed a similar pattern but only from 20 to 30 °C, since the lipid accumulation was reduced at 35 °C. For *U. vinacea*, changes in temperature from 20 to 30 °C showed a positive correlation with PC1 and PC2, indicating enrichment of lipids and proteins. *L. corymbifera* showed an increase in lipids from 20 to 35 °C, which is optimal for growth, followed by a decrease from 35 to 45 °C.

Additionally, Raman spectroscopy complemented the FTIR spectra analysis. Raman spectroscopy provides stronger signals for chemical groups with high polarization, for example, double bonds of carotenoids, making its detection more sensitive. Some species of Mucoromycota, such as *M. circinelloides*, can accumulate significant amounts of carotenoids. Figure 3 shows the Raman spectra of both *M. circinelloides* strains cultivated on MEA at 25, 30, and 35 °C. Carotenoid-related signals at 1525 (C=C stretching, associated with conjugation length), 1155 (C–C stretching and -CH deformation), and 1006 cm⁻¹ (C–CH₃ rocking) [66] showed increased intensities as the growth temperature increased. Based on the intensity of these peaks, out of the two *M. circinelloides* strains, the MC strain was a better carotenoid producer than the MCVI strain, which is in agreement with the findings of previous studies [45]. Increased production of carotenoids with temperature was previously reported for several species of *Mucor* [67, 68], presumably to control oxidative damage and membrane fluidity [69]. However, we cannot ignore the fact that this effect could also be linked to aerial hyphal development and exposure to the air interface. For instance, in *Neurospora crassa*

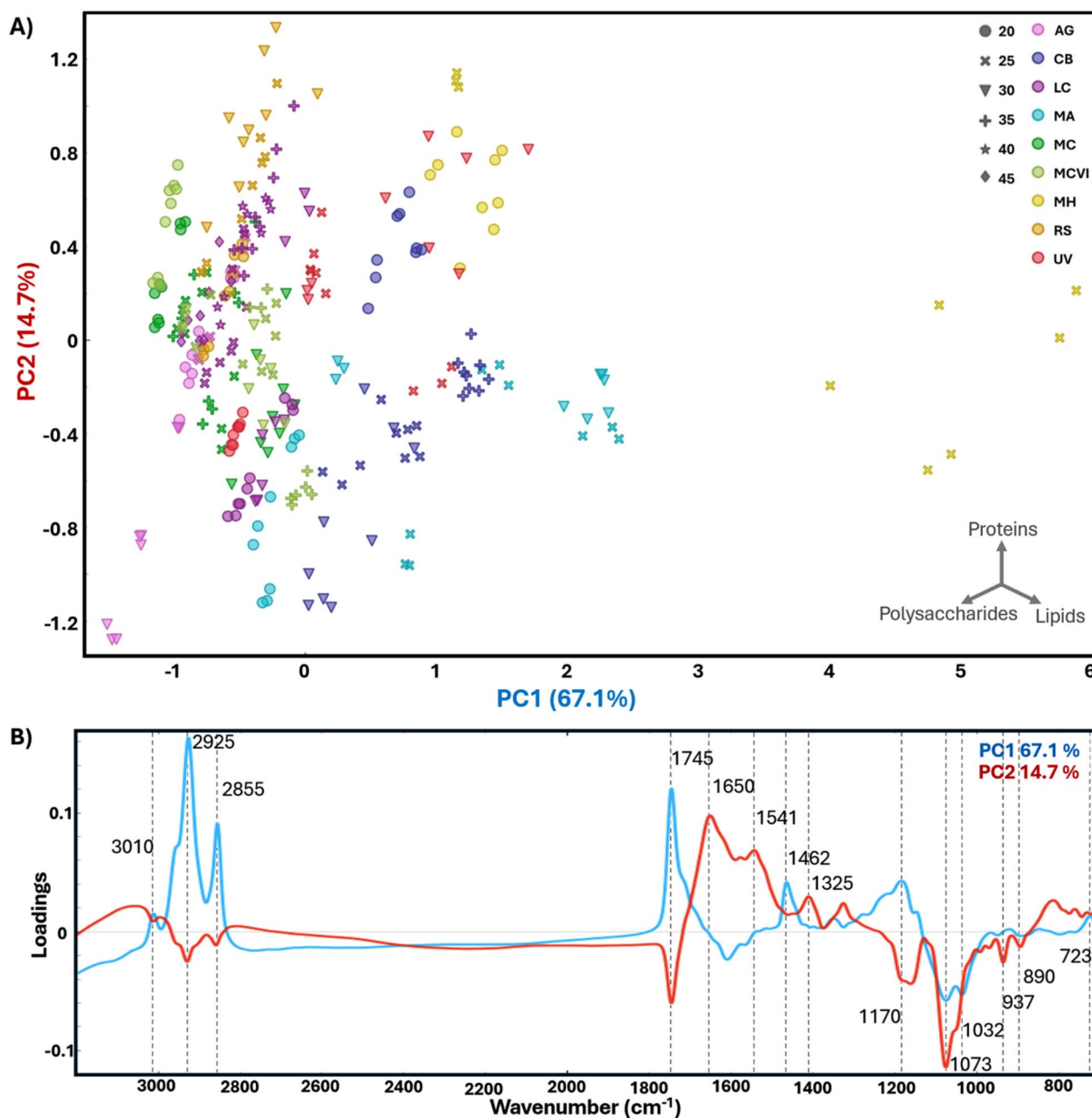


Fig. 2 **A** PCA score plot of the FTIR spectra from the biomass of nine *Mucoromycota* strains grown in MEA at different temperatures. An auxiliary and approximate coordinate vector figure was added to indicate the directions in which the spectra have more contribution to the different metabolites, meaning proteins, polysaccharides, and lipids; **B** loading plots of the first and second principal components (PC1 and PC2) that represented the 67.1% and 14.7% of the total variance

showed that exposition to air is a relevant factor for light-inducible carotenoids [70], controlled by the white-collar complex (WCC) which is widely conserved in the kingdom Fungi, including *M. circinelloides* [71]. Therefore, similar results could not be necessarily translated to submerged fermentation because of the differences in light and air exposition compared to solid media.

Effect of temperature on the lipid profile

Due to our particular interest in lipids, changes in lipids related to incubation temperature were studied in more detail. For this purpose, the lipid-to-protein and unsaturation ratios were calculated from FTIR spectra and are presented below.

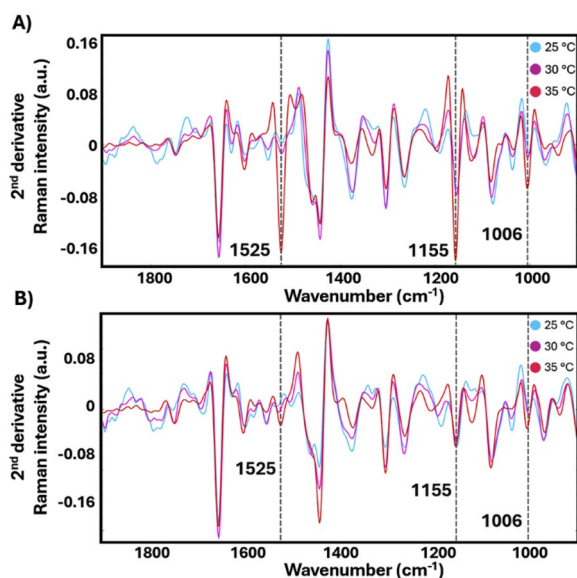


Fig. 3 Raman spectra of mycelium grown on MEA at 25 °C (blue), 30 °C (magenta), and 35 °C (red) from the strains **A)** *M. circinelloides* (MC), and **B)** *M. circinelloides* (MCVI). Carotenoid peaks are marked at 1525, 1155, and 1006 cm^{-1} . Note that the spectra were preprocessed with the 2 second derivative; therefore, the peaks are displayed upside down. The shown spectra are the average of three biologically independent replicates

Previous studies have reported that there are no general correlations between growth temperature and unsaturation and lipid accumulation in some fungi and that the effect of temperature on these parameters is often species-specific [72]. On the other hand, it is generally assumed that the degree of unsaturation of lipids is affected by temperature since unsaturation affects the fluidity of oils and modulates their ability to adapt to different temperatures. In addition, it is also known that the activity of desaturases is regulated by temperature. Understanding the changes in unsaturation levels with temperature for each strain is of interest for the final application of the oil. For example, if oil is used for biodiesel production, a low amount of unsaturated fatty acids is required [11, 73, 74]. Figure 4A shows the lipid-to-protein ratios for each species and incubation temperature, where *M. alpina*, *M. hyalina*, *M. circinelloides*, *U. vinacea*, and *C. blackesleeana* strains did not accumulate substantial amounts of lipids at 20 °C. These results could be related to the slow metabolic activity at this temperature. Therefore, the biomass incubated at 20 °C was not considered to study the correlation between unsaturation and temperature in these strains.

M. alpina and *M. hyalina* had the highest unsaturation ratios (Fig. 4B). This is expected since *Mortierella* fungi are well known for their ability to produce C20 polyunsaturated fatty acids such as arachidonic acid (C20:4n6,

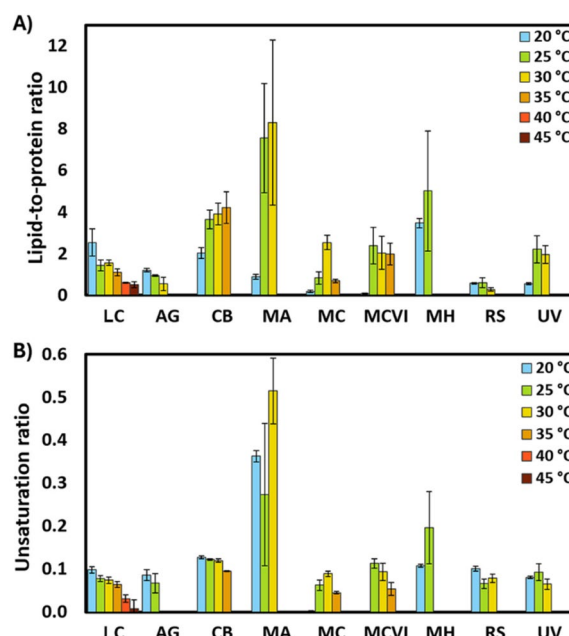


Fig. 4 **A** Lipid-to-protein ratio and **B** unsaturation ratio determined from the FTIR spectra of fungal biomass obtained from the thermal tolerance experiment. Error bars represent the standard deviation of three biologically independent replicates

ARA), dihomogamma-linolenic acid (C20:3n6, DGLA) and eicosapentaenoic acid (20:5n3, EPA) [11, 75]. The lowest unsaturation ratio values were for *A. glauca* and *R. stolonifer*. A progressive decrease in unsaturation with increased temperature was observed for *L. corymbifera*. This is particularly important because *L. corymbifera* could be cultivated at high temperatures during the SSF process, resulting in a higher hydrolysis efficiency and oil with more favorable characteristics for biodiesel production than at lower temperatures [76]. For both *M. circinelloides* strains, there was a significant decrease of unsaturation observed at 35 °C. In contrast, for *U. vinacea* and *C. blackesleeana* the unsaturation remained almost unchanged from 20 to 30 °C, and a slight decrease in unsaturation was detected for *C. blackesleeana* at 35 °C.

Cellulase induction by the presence of cellobiose and cellulose

Most of the studied Mucoromycota strains grew well in the cellobiose-based medium except *M. alpina* and *M. hyalina* (Fig. 5A). Modifications in the medium, such as supplementation with the vitamins biotin (0.02 mg/L) and thiamine hydrochloride (0.05 g/L) or yeast extract as the sole nitrogen source, did not change the inability of these species to grow in cellobiose medium (data not shown). This could be related to the absence of metabolic

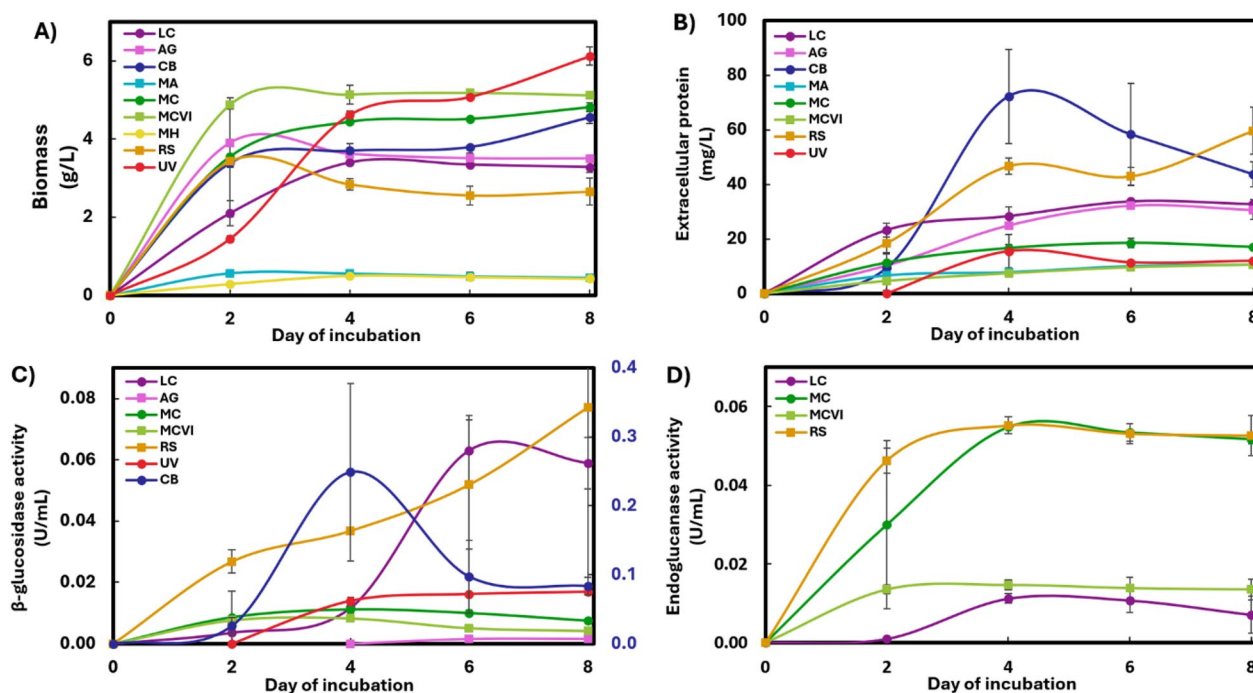


Fig. 5 **A** Biomass growth, **B** extracellular protein, **C** β -glucosidase activity, and **D** endoglucanase activity of the nine Mucoromycota strains cultivated in cellobiose-based medium. Note that the β -glucosidase activity of the *C. blakesleeana* (CB) strain is displayed on the secondary y-axis due to its large values compared to those of the other strains. Error bars represent the standard deviation of three biologically independent replicates

tools for cellobiose uptake. Although it has been reported that *Mortierella isabellina* can grow in a medium with a similar composition and cellobiose as a carbon source [77], it must be stated that this species is no longer a valid member of the *Mortierella* genus being nowadays named as *Umbelopsis isabellina* [78]. *Mortierella* is a genus with strong associations with rhizosphere and endophytic plant interactions [79]; therefore, it might be that these species have a reduced amount of plant cell wall degrading enzymes or do not react upon intermediaries of cellulose, such as cellobiose, to avoid plant defense response [80, 81].

Additionally, *L. corymbifera* was grown at 35 °C, near its optimal for growth, since at 25 °C the growth was delayed until 6 days and the levels of biomass, extracellular protein, and enzymatic activity were so low that could not be analyzed properly (data not shown).

Almost all the strains started to grow before the maximum level of extracellular protein was reached (Fig. 5B). This indicates that most of the strains can take up cellobiose by membrane transporters and process it intracellularly before the expression of extracellular β -glucosidase. For instance, it was reported that *M. circinelloides* has intracellular and extracellular β -glucosidases [32], which could be also the case for the other studied Mucoromycota strains. In contrast,

the growth of *U. vinacea* and *L. corymbifera* seemed to depend more on enzyme expression since their exponential growth phase overlapped with the maximum peak of extracellular protein expression on day 4 and day 6, respectively.

All the strains, except *M. alpina* and *M. hyalina*, secreted extracellular proteins with β -glucosidase activity at different times and magnitudes (Fig. 5C). The highest values of β -glucosidase activity were found in *C. blakesleeana*, *R. stolonifer*, and *L. corymbifera* reaching a maximum of 0.25 U/mL on day 4, 0.084 U/mL on day 8, and 0.063 U/mL on day 6, respectively. The expression of β -glucosidase in *U. vinacea* was low and started between day 2 and day 4 of incubation, aligned with the exponential growth phase of the fungus. It seems that, for *U. vinacea*, the processing of cellobiose is predominantly extracellular. This observation could be related to the reduced size of the genome and membrane transporters of the genus *Umbelopsis* compared to those of other *Mucorales* [82]. *A. glauca* showed good growth, although it is interesting to note that, even though the values of extracellular protein were significantly high from day 2 of incubation (10.18 mg/L), the β -glucosidase activity remained low. This observation could be related to a low affinity for the p-NPG substrate used in the enzymatic activity assay or the expression of other enzymes with

different activities since the specific activity was relatively low (Fig. 6B).

As stated in previous studies, there are scarce studies of β -glucosidase in Mucoromycota, and this topic deserves additional attention due to the potential applicability of Mucoromycota in SSF processes [83]. The expression of β -glucosidase induced by cellobiose was studied for several species of the genera *Mucor*, *Gilbertella*, *Rhizomucor*, and *Rhizopus* [33]. The *Rhizopus* genus had the highest activity, namely, *R. oryzae* and *R. stolonifer*, followed by one strain of *Mucor miehei* and three strains of

Gilbertella persicaria. In our study, the detailed response to cellobiose was studied not only for *Mucor circinelloides* and *Rhizopus stolonifer*, but also for other Mucoromycota species, like *Lichtheimia corymbifera*, *Cunninghamella blackesleeana*, *Absidia glauca*, *Umbelopsis vinacea*, *Mortierella hyalina* and *Mortierella alpina*. Special attention should be given to *Cunninghamella blackesleeana*, a species that outperformed the other strains in terms of β -glucosidase expression with high specific activity in the extracellular protein secreted (Fig. 6B).

When it comes to endoglucanase expression in the cellobiose-based medium, only *R. stolonifer*, *M. circinelloides*, *M. circinelloides* VI, and *L. corymbifera* showed activity beginning on day 2 of incubation (Fig. 5D). Thus, both *Mucor*, *Rhizopus*, and *Lichtheimia* strains showed cellobiose-triggered expression of both endoglucanase and β -glucosidase. This observation aligns with the fact that *M. circinelloides* and *R. stolonifer* species are common in postharvest infections of fruits and vegetables [84, 85], and *L. corymbifera* is commonly associated with dead plant material niches [86, 87], where these enzymes facilitate infection by enabling access to plant material [32, 88, 89]. In particular, *R. stolonifer* displayed notably high activities for both endoglucanase and β -glucosidase in the presence of cellobiose. The regulatory system for cellulase expression in *R. stolonifer* was studied previously, which depends on a cellobiose-responsive regulator [90]. Regarding *M. circinelloides*, although there are studies about the induction of endoglucanase using CMC [32], to the best of the author's knowledge, there are no reports in the literature about the induction of endoglucanase expression by cellobiose; and the same for the case of *L. corymbifera*.

Additionally, for the strains that were able to grow in the presence of cellobiose, a decrease in the pH of the supernatant was observed along with growth in the exponential phase (Fig. 6A). This indicates the production of CO_2 and/or acids due to the consumption of cellobiose. In particular, a large decrease in pH was observed for *A. glauca* from pH 6.6 to 3.5, indicating either abundant secretion of acid or moderate production of an acid with a low pKa. To the best of the authors' knowledge, acid production by *A. glauca* has not been reported in the literature. In the later stages of growth, the pH increase coincided with the maximum amount of extracellular protein secretion, possibly due to the buffering effect of the protein.

When Mucoromycota strains were cultivated in cellulose-based medium, extracellular proteins were detected for all the strains except *M. hyalina* and *U. vinacea*, with the highest values observed for *R. stolonifer* and *M. alpina* (Fig. 7A). β -Glucosidase activity was detected in all the strains, except for *M. alpina*,

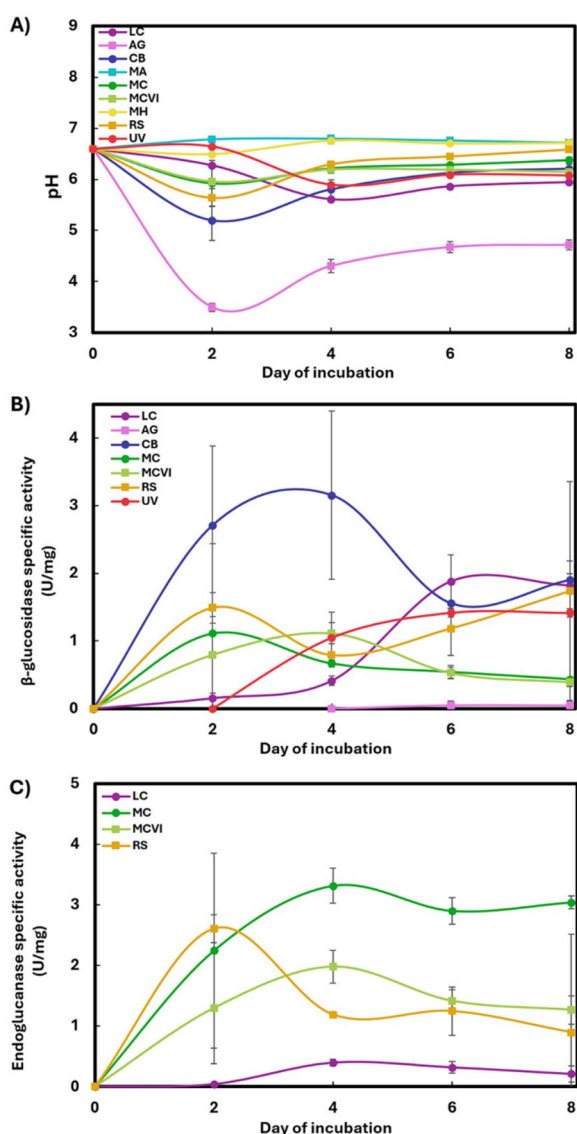


Fig. 6 A pH, B β -glucosidase specific activity, and C endoglucanase specific activity values of the nine Mucoromycota strains cultivated in the cellobiose-based medium. Error bars represent the standard deviation of three biologically independent replicates

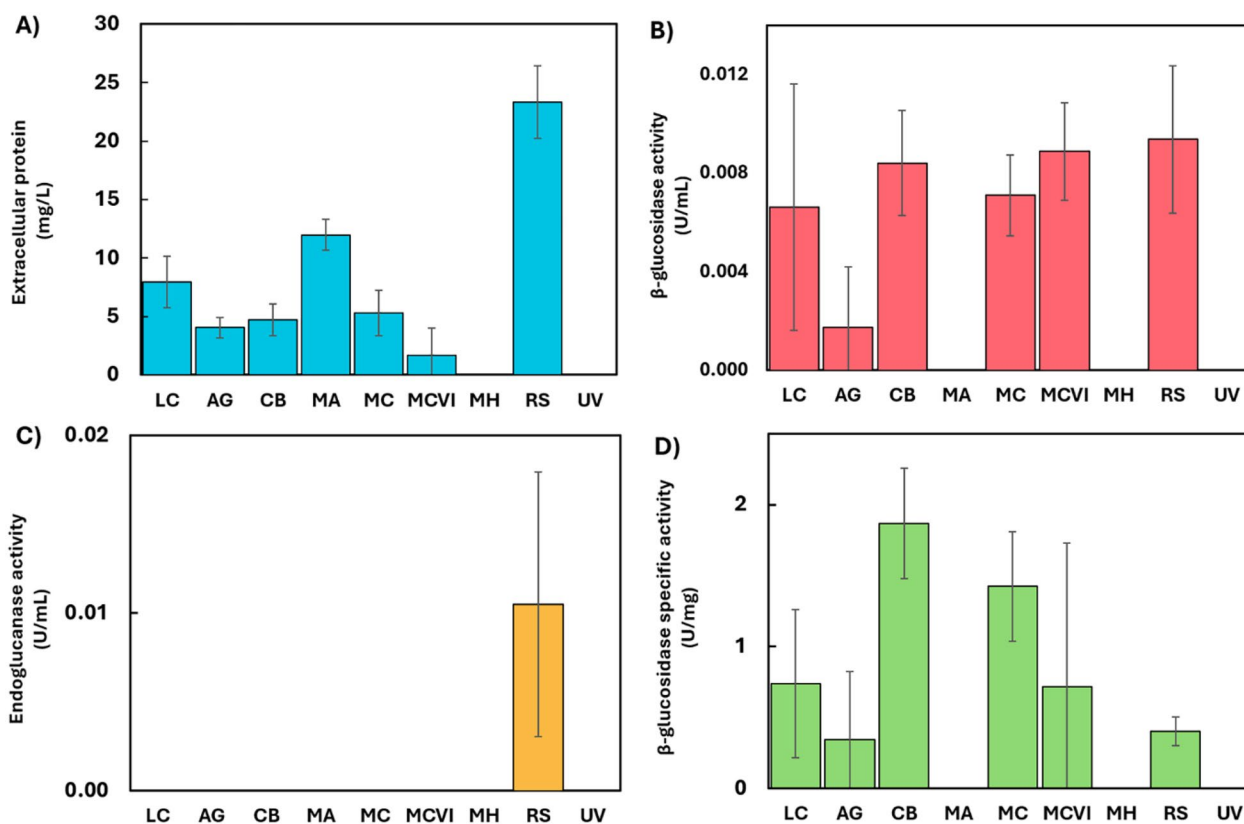


Fig. 7 A Extracellular protein, B β -glucosidase activity, C endoglucanase activity, and D β -glucosidase specific activity in the supernatants of the nine Mucoromycota strains grown in cellulose-based medium. Error bars represent the standard deviation of three biologically independent replicates

M. hyalina, and *U. vinacea* (Fig. 7B), while the endoglucanase activity was only detected for *R. stolonifer* (Fig. 7C). However, these values were lower than in the cellobiose-based medium experiment. The highest β -glucosidase activities observed were for *R. stolonifer* and both *M. circinelloides* strains. Surprisingly, although *M. alpina* had the second highest value of extracellular protein, β -glucosidase activity was not detected. This could indicate the expression of other type of enzymes or proteins or the occurrence of cellular apoptosis. High variability in β -glucosidase activity was obtained for *L. corymbifera* and *A. glauca* because the values were near the detection limit of the method. When it comes to the specific activity, *C. blakesleeana* was the strain with the highest values, followed by *M. circinelloides* and *M. circinelloides* VI. Once more, *C. blakesleeana* showed to either express pure β -glucosidase or several extracellular proteins with highly active β -glucosidases (Fig. 7D).

To sum up, the induction of cellulases by cellobiose and cellulose was studied in depth for representative species in Mucoromycota not studied before. Except for *M. hyalina* and *M. alpina*, the tested strains seemed to be

favorable for SSF processes where the accumulation of cellobiose could be a problem.

Conclusions

This study reports a comprehensive analysis of key traits identified as important for a successful SSF using oleaginous Mucoromycota species. Among the studied Mucoromycota, *L. corymbifera* was the most suitable for SSF. Future works will study the development of SSF with the best candidates of this work addressing its strengths and weaknesses.

FTIR and Raman spectroscopy provided rich information on the whole biochemical composition of the fungal biomass. The fast acquisition and minimal sample preparation for these techniques allowed us to study the effect of temperature on fungal biomass composition such as lipid saturation.

Certain traits of *R. stolonifer* that could be related to its great ability to infect and spoil fruits, vegetables, and other foods were found in this study. These include fast growth extension of mycelium, induced expression of endoglucanase and β -glucosidase by cellobiose and cellulose, and production of large amounts of acid, such

as fumaric and lactic acid [91]. These properties enable *R. stolonifer* to outcompete other fungi by settling and extending fast and macerating vegetable material with acids and enzymes for posterior infection and access to nutrients.

Supplementary Information

The online version contains supplementary material available at <https://doi.org/10.1186/s13068-025-02621-w>.

Additional file 1

Acknowledgements

Not applicable.

Author contributions

Conceived the research idea: CBL, BZ, AK, VS. Designed the experiments: CBL. Methodology: CBL, VS, BZ. Performed the experiment: CBL, OS, DB. Discussed the results: CBL, OS, DB, BZ, SJH, AK, VS. Analyzed the data: CBL, BZ. Wrote the manuscript: CBL. Discussed and revised the manuscript: CBL, OS, DB, BZ, SJH, AK, VS. All authors read and approved the final manuscript.

Funding

This work was supported by the Research Council of Norway [FMETEK-N-FME grant number 257622 (Bio4Fuels), BIONÆR grant number 305215, DAAD grant number 309220; HAVBRUK2 grant number 302543/E40, MATFONDAVTALE grant number 301834/E50].

Availability of data and materials

The datasets supporting the conclusions of this article are available in the Zenodo repository at <https://doi.org/https://doi.org/10.5281/zenodo.13838385>. Data indicated as "Data not shown" are made available on request.

Declarations

Ethics approval and consent to participate

Not applicable.

Consent for publication

Not applicable.

Competing interests

The authors declare no competing interests.

Author details

¹Faculty of Science and Technology, Norwegian University of Life Sciences (NMBU), 1433 Ås, Norway. ²Faculty of Chemistry, Biotechnology and Food Sciences, Norwegian University of Life Sciences (NMBU), 1433 Ås, Norway.

Received: 26 September 2024 Accepted: 11 February 2025

Published online: 24 February 2025

References

- Ratledge C. Microbial oils and fats: an assessment of their commercial potential. *Prog Ind Microbiol*. 1982;16:119–206.
- Dzurenkova S, Zimmermann B, Tafintseva V, Kohler A, Ekeberg D, Shapaval V. The influence of phosphorus source and the nature of nitrogen substrate on the biomass production and lipid accumulation in oleaginous Mucoromycota fungi. *Appl Microbiol Biotechnol*. 2020;104(18):8065–76.
- Wältermann M, Steinbüchel A. Neutral lipid bodies in prokaryotes: recent insights into structure, formation, and relationship to eukaryotic lipid depots. *J Bacteriol*. 2005;187(11):3607–19.
- Slocombe SP, Zhang Q, Ross M, Anderson A, Thomas NJ, Lapresa Á, et al. Unlocking nature's treasure-chest: screening for oleaginous algae. *Sci Rep*. 2015;5:1–17.
- Byrtusová D, Shapaval V, Holub J, Šimanský S, Rapta M, Sztokowski M, et al. Revealing the potential of lipid and β -coproduction in basidiomycetes yeast. *Microorganisms*. 2020;8(7):1–19.
- Olsen PM, Kósa G, Klüver M, Kohler A, Shapaval V, Horn SJ. Production of docosahexaenoic acid from spruce sugars using Aurantiochytrium limacinum. *Bioresour Technol*. 2023. <https://doi.org/10.1016/j.biortech.2023.128827>.
- Subramaniam R, Dufreche S, Zappi M, Bajpai R. Microbial lipids from renewable resources: production and characterization. *J Ind Microbiol Biotechnol*. 2010;37(12):1271–87.
- Kosa M, Ragauskas AJ. Lipids from heterotrophic microbes: Advances in metabolism research. *Trends Biotechnol*. 2011;29(2):53–61. <https://doi.org/10.1016/j.tibtech.2010.11.002>.
- Jin M, Slininger PJ, Dien BS, Waghmode S, Moser BR, Orjuela A, et al. Microbial lipid-based lignocellulosic biorefinery: feasibility and challenges. *Trends Biotechnol*. 2015;33(1):43–54. <https://doi.org/10.1016/j.tibtech.2014.11.005>.
- Wynn JP, Hamid AA, Li Y, Ratledge C. Biochemical events leading to the diversion of carbon into storage lipids in the oleaginous fungi *Mucor circinelloides* and *Mortierella alpina*. *Microbiology*. 2001;147(10):2857–64.
- Kosa G, Zimmermann B, Kohler A, Ekeberg D, Afseth NK, Mounier J, et al. High-throughput screening of Mucoromycota fungi for production of low- and high-value lipids. *Biotechnol Biofuels*. 2018;11(1):1–17. <https://doi.org/10.1186/s13068-018-1070-7>.
- Zhao H, Lv M, Liu Z, Zhang M, Wang Y, Ju X, et al. High-yield oleaginous fungi and high-value microbial lipid resources from Mucoromycota. *Bioenergy Res*. 2021;14(4):1196–206.
- Ratledge C. Microbial production of gamma-linolenic acid. Boca Raton, USA: CRC Press; 2006.
- Mamani LDG, Magalhães AI, Ruan Z, de Carvalho JC, Soccol CR. Industrial production, patent landscape, and market trends of arachidonic acid-rich oil of *Mortierella alpina*. *Biotechnol Res Innov*. 2019;3(1):103–19. <https://doi.org/10.1016/j.biori.2019.02.002>.
- Hannula SE, Jongen R, Morriën E. Grazing by collembola controls fungal induced soil aggregation. *Fungal Ecol*. 2023;65:101284.
- Dzurenkova S, Losada CB, Dupuy-Galet BX, Fjær K, Shapaval V. Mucoromycota fungi as powerful cell factories for modern biorefinery. *Appl Microbiol Biotechnol*. 2022. <https://doi.org/10.1007/s00253-021-11720-1>.
- Gaykawad SS, Ramanand SS, Blomqvist J, Zimmermann B, Shapaval V, Kohler A, et al. Submerged fermentation of animal fat by-products by oleaginous filamentous fungi for the production of unsaturated single cell oil. *Fermentation*. 2021. <https://doi.org/10.3390/fermentation7040300>.
- Slány O, Klempová T, Shapaval V, Zimmermann B, Kohler A, Čertík M. Animal fat as a substrate for production of n-6 fatty acids by fungal solid-state fermentation. *Microorganisms*. 2021;9(1):1–17.
- Liu G, Zhang J, Bao J. Cost evaluation of cellulase enzyme for industrial-scale cellulosic ethanol production based on rigorous Aspen Plus modeling. *Bioprocess Biosyst Eng*. 2016;39(1):133–40.
- Karimi K, Emthiaz G, Taherzadeh MJ. Ethanol production from dilute-acid pretreated rice straw by simultaneous saccharification and fermentation with *Mucor indicus*, *Rhizopus oryzae*, and *Saccharomyces cerevisiae*. *Enzyme Microb Technol*. 2006;40(1):138–44.
- Sudiyani Y, Dahnum D, Burhani D, Putri AMH. Evaluation and comparison between simultaneous saccharification and fermentation and separated hydrolysis and fermentation process. In: Basile A, Dalena F, editors. *Second and Third Generation of Feedstocks: The Evolution of Biofuels*. Elsevier Inc: Amsterdam; 2019. p. 273–90.
- Johnson E. Integrated enzyme production lowers the cost of cellulosic ethanol. *Biofuels, Bioprod Biorefining*. 2016;10(2):164–74.
- Kazi FK, Fortman J, Anex R, Kothandaraman G, Hsu D, Aden A, et al. Techno-Economic Analysis of Biochemical Scenarios for Production of Cellulosic Ethanol Techno-Economic Analysis of Biochemical Scenarios for Production of Cellulosic Ethanol. NREL/TP-6A2-46588. 2010. Available from: NREL/TP-6A2-46588
- Clariant. Converting straw to advanced biofuels with sunliquid®. 2023. Clariant. <https://www.clariant.com/en/Business-Units/Catalysts/Sunliquid>
- Rødstrud G, Lersch M, Sjöde A. History and future of world's most advanced biorefinery in operation. *Biomass Bioenerg*. 2012;46:46–59.

26. Bischof RH, Ramoni J, Seiboth B. Cellulases and beyond: the first 70 years of the enzyme producer *Trichoderma reesei*. *Microb Cell Fact*. 2016;15(1):1–13.
27. Humbird D, Davis R, Tao L, Kinchin C, Hsu D, Aden A, et al. Process design and economics for biochemical conversion of lignocellulosic biomass to ethanol: dilute-acid pretreatment and enzymatic hydrolysis of corn stover. National Renewable Energy Laboratory. NREL/TP-5100-47764. 2011.
28. Sørensen A, Teller PJ, Lübeck PS, Ahring BK. Onsite enzyme production during bioethanol production from biomass: Screening for suitable fungal strains. *Appl Biochem Biotechnol*. 2011;164(7):1058–70.
29. Mach RL, Seiboth B, Myasnikov A, Gonzalez R, Strauss J, Harkki AM, et al. The *bgl1* gene of *Trichoderma reesei* QM 9414 encodes an extracellular, cellulose-inducible β -glucosidase involved in cellulase induction by sophorose. *Mol Microbiol*. 1995;16(4):687–97.
30. Sørensen A, Lübeck M, Lübeck PS, Ahring BK. Fungal beta-glucosidases: a bottleneck in industrial use of lignocellulosic materials. *Biomolecules*. 2013;3(3):612–31.
31. Huang Y, Busk PK, Grell MN, Zhao H, Lange L. Identification of a β -glucosidase from the *Mucor circinelloides* genome by peptide pattern recognition. *Enzyme Microb Technol*. 2014;67:47–52. <https://doi.org/10.1016/j.enzmictec.2014.09.002>.
32. Wei H, Wang W, Yarbrough JM, Baker JO, Laurens L, van Wycken S, et al. Genomic, proteomic, and biochemical analyses of oleaginous *Mucor circinelloides*: evaluating its capability in utilizing cellulosic substrates for lipid production. *PLoS ONE*. 2013;8(9):1–12.
33. Takó M, Farkas E, Lung S, Krisch J, Vágvolgyi C, Papp T. Identification of acid- and thermotolerant extracellular β -glucosidase activities in *Zygomycetes* fungi. *Acta Biol Hung*. 2010;61(1):101–10.
34. Hüttner S, Granchi Z, Nguyen TT, van Pelt S, Larsbrink J, Thanh VN, et al. Genome sequence of *Rhizomucor pusillus* FCH 5.7, a thermophilic zygomycete involved in plant biomass degradation harbouring putative GH9 endoglucanases. *Biotechnol Reports*. 2018. <https://doi.org/10.1016/j.btre.2018.e00279>.
35. Shimonaka A, Koga J, Baba Y, Nishimura T, Murashima K, Kubota H, et al. Specific characteristics of family 45 endoglucanases from mucorales in the use of textiles and laundry. *Biosci Biotechnol Biochem*. 2006;70(4):1013–6.
36. Tang H, Hou J, Shen Y, Xu L, Yang H, Fang X, et al. High β -glucosidase secretion in *Saccharomyces cerevisiae* improves the efficiency of cellulase hydrolysis and ethanol production in simultaneous saccharification and fermentation. *J Microbiol Biotechnol*. 2013;23(11):1577–85.
37. Zou S, Jia Y, He Q, Zhang K, Ban R, Hong J, et al. Comparison of the unfolded protein response in cellobiose utilization of recombinant *angel*- and *W303-1A*-derived yeast expressing β -glucosidase. *Front Bioeng Biotechnol*. 2022;10(March):1–13.
38. Vasylyshyn R, Dmytruk O, Sybirnyy A, Ruchala J. Engineering of *Ogataea polymorpha* strains with ability for high-temperature alcoholic fermentation of cellobiose. *FEMS Yeast Res*. 2024. <https://doi.org/10.1093/femsyr/foae007>.
39. Kim H, Oh EJ, Lane ST, Lee WH, Cate JHD, Jin YS. Enhanced cellobiose fermentation by engineered *Saccharomyces cerevisiae* expressing a mutant cellodextrin facilitator and cellobiose phosphorylase. *J Biotechnol*. 2018;275:53–9. <https://doi.org/10.1016/j.jbiotec.2018.04.008>.
40. Szotkowski M, Byrtusova D, Haronikova A, Vysoka M, Rapta M, Shapaval V, et al. Study of metabolic adaptation of red yeasts to waste animal fat substrate. *Microorganisms*. 2019. <https://doi.org/10.3390/microorganisms7110578>.
41. Ha SJ, Kim H, Lin Y, Jang MU, Galazka JM, Kim TJ, et al. Single amino acid substitutions in HXT2.4 from *Scheffersomyces stipitis* lead to improved cellobiose fermentation by engineered *Saccharomyces cerevisiae*. *Appl Environ Microbiol*. 2013;79(5):1500–7.
42. Lewis Liu Z, Weber SA, Cotta MA, Li SZ. A new β -glucosidase producing yeast for lower-cost cellulosic ethanol production from xylose-extracted corn cob residues by simultaneous saccharification and fermentation. *Bioresour Technol*. 2012;104:410–6.
43. Olofsson K, Bertilsson M, Lidén G. A short review on SSF - an interesting process option for ethanol production from lignocellulosic feedstocks. *Biotechnol Biofuels*. 2008;1:1–14.
44. Kosa G, Kohler A, Tafintseva V, Zimmermann B, Forfang K, Afseth NK, et al. Microtiter plate cultivation of oleaginous fungi and monitoring of lipogenesis by high-throughput FTIR spectroscopy. *Microb Cell Fact*. 2017;16(1):1–12.
45. Dzurendova S, Zimmermann B, Kohler A, Reitzel K, Nielsen UG, Dupuy-galet BX, et al. Calcium affects polyphosphate and lipid accumulation in *Mucoromycota* fungi. *J Fungi*. 2021. <https://doi.org/10.3390/jof7040300>.
46. Dzurendova S, Zimmermann B, Kohler A, Tafintseva V, Slany O, Certik M, et al. Microcultivation and FTIR spectroscopy-based screening revealed a nutrient-induced co-production of high-value metabolites in oleaginous *Mucoromycota* fungi. *PLoS ONE*. 2020. <https://doi.org/10.1371/journal.pone.0234870>.
47. Dzurendová S, Shapaval V, Tafintseva V, Kohler A, Byrtusová D, Szotkowski M, et al. Assessment of biotechnologically important filamentous fungal biomass by Fourier transform Raman spectroscopy. *Int J Mol Sci*. 2021;22(13):6710.
48. Hu KJ, Hu JL, Ho KP, Yeung KW. Screening of fungi for chitosan producers, and copper adsorption capacity of fungal chitosan and chitosanaceous materials. *Carbohydr Polym*. 2004;58(1):45–52.
49. Lee SC, Li A, Calo S, Heitman J. Calcineurin plays key roles in the dimorphic transition and virulence of the human pathogenic zygomycete *Mucor circinelloides*. *PLoS Pathog*. 2013;9(9):1003625.
50. Dzurendova S, Zimmermann B, Tafintseva V, Kohler A, Horn SJ, Shapaval V. Metal and phosphate ions show remarkable influence on the biomass production and lipid accumulation in oleaginous *Mucor circinelloides*. *J Fungi*. 2020;6(4):1–23.
51. Das RK, Brar SK, Verma M. Fumaric Acid: production and applications aspects. In: Brar SK, Sarma SJ, Pakshirajan K, editors. *Platform Chemical Biorefinery: Future Green Chemistry*. Elsevier: Amsterdam; 2016. p. 133–57.
52. Trinci A. A kinetic study of the growth of *Aspergillus nidulans* and other fungi. *J Gen Microbiol*. 1969;57:11–24.
53. Ernst O, Zor T. Linearization of the Bradford protein assay. *J Vis Exp*. 2010;38:1–6.
54. Sonia KG, Chadha BS, Badhan AK, Saini HS, Bhat MK. Identification of glucose tolerant acid active β -glucosidases from thermophilic and thermotolerant fungi. *World J Microbiol Biotechnol*. 2008;24(5):599–604.
55. Samira M, Mohammad R, Gholamreza G. Carboxymethyl-cellulase and filter-paperase activity of new strains isolated from persian gulf. *Microbiol J*. 2011;1(1):8–16.
56. Zimmermann B, Kohler A. Optimizing Savitzky-Golay parameters for improving spectral resolution and quantification in infrared spectroscopy. *Appl Spectrosc*. 2013;67(8):892–902.
57. Guo S, Kohler A, Zimmermann B, Heinke R, Stöckel S, Rösch P, et al. Extended multiplicative signal correction based model transfer for Raman spectroscopy in biological applications. *Anal Chem*. 2018;90(16):9787–95.
58. Demšar J, Curk T, Erjavec A, Gorup Č, Hočevar T, Milutinovič M, et al. Orange: data mining toolbox in python. *J Mach Learn Res*. 2013;14:2349–53.
59. Toplak M, Birarda G, Read S, Sandt C, Rosendahl SM, Vaccari L, et al. Infrared orange: connecting hyperspectral data with machine learning. *Synchrotron Radiat News*. 2017;30(4):40–5.
60. Snowdon AL. A colour atlas of post-harvest diseases and disorders of fruits and vegetables. London UK: Wolfe Scientific Ltd; 1990.
61. Hoffmann K, Discher S, Voigt K, Hawksworth DL. Revision of the genus *Absidia* (*Mucorales*, *Zygomycetes*) based on physiological, phylogenetic, and morphological characters; thermotolerant *Absidia* spp. form a coherent group *Mycocladaceae* fam. nov. *Mycol Res*. 2007;111:169–83.
62. Galbe M, Wallberg O, Zacchi G. *Techno-Economic Aspects of Ethanol Production from Lignocellulosic Agricultural Crops and Residues*. Amsterdam: Elsevier BV; 2011.
63. Conti E, Stredanska M, Stredanska S, Zanetti F. γ -Linolenic acid production by solid-state fermentation of *Mucorales* strains on cereals. *Bioresour Technol*. 2001;76(3):283–6.
64. Xin F, Dang W, Chang Y, Wang R, Yuan H, Xie Z, et al. Transcriptomic analysis revealed the differences in lipid accumulation between spores and mycelia of *Mucor circinelloides* WJ11 under Solid-State Fermentation. *Fermentation*. 2022. <https://doi.org/10.3390/fermentation8120667>.
65. Tang X, Chen H, Chen YQ, Chen W, Garre V, Song Y, et al. Comparison of biochemical activities between high and low lipid-producing strains of *Mucor circinelloides*: an explanation for the high oleaginicuity of strain WJ11. *PLoS ONE*. 2015;10(6):1–12.

66. Britton G, Llaaen-Jensen S, Pfander H. Carotenoids. Berlin: Birkhäuser Verlag; 2008.
67. Dexter Y, Cooke RC. Fatty acids, sterols and carotenoids of the psychrophile *Mucor strictus* and some mesophilic *Mucor* species. *Trans Br Mycol Soc.* 1984;83(3):455–61. [https://doi.org/10.1016/S0007-1536\(84\)80041-8](https://doi.org/10.1016/S0007-1536(84)80041-8).
68. Mosqueda-Cano G, Gutiérrez-Corona JF. Environmental and developmental regulation of carotenogenesis in the dimorphic fungus *Mucor rouxii*. *Curr Microbiol.* 1995;31(3):141–5.
69. McNulty HP, Byun J, Lockwood SF, Jacob RF, Mason RP. Differential effects of carotenoids on lipid peroxidation due to membrane interactions: X-ray diffraction analysis. *Biochim Biophys Acta - Biomembr.* 2007;1768(1):167–74.
70. Iigusa H, Yoshida Y, Hasunuma K. Oxygen and hydrogen peroxide enhance light-induced carotenoid synthesis in *Neurospora crassa*. *FEBS Lett.* 2005;579(18):4012–6.
71. Silva F, Torres-Martínez S, Garre V. Distinct white collar-1 genes control specific light responses in *Mucor circinelloides*. *Mol Microbiol.* 2006;61(4):1023–37.
72. Suutari M. Effect of growth temperature on lipid fatty acids of four fungi (*Aspergillus niger*, *Neurospora crassa*, *Penicillium chrysogenum*, and *Trichoderma reesei*). *Arch Microbiol.* 1995;164(3):212–6.
73. Stansell GR, Gray VM, Sym SD. Microalgal fatty acid composition: implications for biodiesel quality. *J Appl Phycol.* 2012;24(4):791–801.
74. Patel A, Karageorgou D, Rova E, Katapodis P, Rova U, Christakopoulos P, et al. An overview of potential oleaginous microorganisms and their role in biodiesel and omega-3 fatty acid-based industries. *Microorganisms.* 2020;8(3):1–39.
75. Weete JD, Gandhi SR. Sterols and fatty acids of the Mortierellaceae: taxonomic implications. *Mycologia.* 1999;91(4):642–9.
76. Ramírez-Verduzco LF, Rodríguez-Rodríguez JE, Jaramillo-Jacob ADR. Predicting cetane number, kinematic viscosity, density and higher heating value of biodiesel from its fatty acid methyl ester composition. *Fuel.* 2012;91(1):102–11.
77. Zeng J, Zheng Y, Yu X, Yu L, Gao D, Chen S. Lignocellulosic biomass as a carbohydrate source for lipid production by *Mortierella isabellina*. *Biore-source Technol.* 2013;128:385–91. <https://doi.org/10.1016/j.biortech.2012.10.079>.
78. Streekstra H. On the safety of *Mortierella alpina* for the production of food ingredients, such as arachidonic acid. *J Biotechnol.* 1997;56(3):153–65.
79. Bonfante P, Venice F. Mucoromycota: going to the roots of plant-interacting fungi. *Fungal Biol Rev.* 2020;34(2):100–13.
80. Kohler A, Kuo A, Nagy LG, Morin E, Barry KW, Buscot F, et al. Convergent losses of decay mechanisms and rapid turnover of symbiosis genes in mycorrhizal mutualists. *Nat Genet.* 2015;47(4):410–5. <https://doi.org/10.1038/ng.3223>.
81. Lebreton A, Corre E, Jany JL, Brillet-Guéguen L, Pérez-Arques C, Garre V, et al. Comparative genomics applied to *Mucor* species with different lifestyles. *BMC Genomics.* 2020;21(1):1–21.
82. Muszewska A, Okrańska A, Steczkiewicz K, Drgas O, Orłowska M, Perlińska-Lenart U, et al. Metabolic potential, ecology and presence of associated bacteria is reflected in genomic diversity of mucoromycotina. *Front Microbiol.* 2021;12(February):1–21.
83. Kato Y, Nomura T, Ogita S, Takano M, Hoshino K. Two new β -glucosidases from ethanol-fermenting fungus *Mucor circinelloides* NBRC 4572: Enzyme purification, functional characterization, and molecular cloning of the gene. *Appl Microbiol Biotechnol.* 2013;97(23):10045–56.
84. Bautista-Baños S, Bosquez-Molina E, Barrera-Necha LL. *Rhizopus stolonifer* (Soft Rot). Amsterdam: Elsevier; 2014.
85. Saito S, Michailides TJ, Xiao CL. *Mucor Rot*—An emerging postharvest disease of mandarin fruit caused by *Mucor piriformis* and other *Mucor* spp. In *California Plant Dis.* 2016;100(6):1054–63.
86. Alastruey-Izquierdo A, Hoffmann K, De Hoog GS, Rodríguez-Tudela JL, Voigt K, Bibashi E, et al. Species recognition and clinical relevance of the zygomycetous genus *Lichtheimia* (syn. *Absidia pro parte*, *Mycocladius*). *J Clin Microbiol.* 2010;48(6):2154–70.
87. Di Piazza S, Houbraken J, Meijer M, Cecchi G, Kraak B, Rosa E, et al. Thermotolerant and thermophilic mycobiota in different steps of compost maturation. *Microorganisms.* 2020;8(6):1–9.
88. Battaglia E, Benoit I, van den Brink J, Wiebenga A, Coutinho PM, Henrissat B, et al. Carbohydrate-active enzymes from the zygomycete fungus *Rhizopus oryzae*: a highly specialized approach to carbohydrate degradation depicted at genome level. *BMC Genomics.* 2011;12:1–2.
89. Petrasch S, Silva CJ, Mesquida-Pesci SD, Gallegos K, van den Abeele C, Papin V, et al. Infection strategies deployed by *Botrytis cinerea*, *Fusarium acuminatum*, and *Rhizopus stolonifer* as a function of tomato fruit ripening stage. *Front Plant Sci.* 2019;10(March):1–17.
90. Zhang Y, Tang B, Du G. Self-induction system for cellulase production by cellobiose produced from glucose in *Rhizopus stolonifer*. *Sci Rep.* 2017;7(1):1–9. <https://doi.org/10.1038/s41598-017-10964-0>.
91. Zaveri A, Edwards J, Rochfort S. Production of primary metabolites by *Rhizopus stolonifer*, causal agent of almond hull rot disease. *Molecules.* 2022. <https://doi.org/10.3390/molecules27217199>.

Publisher's Note

Springer Nature remains neutral with regard to jurisdictional claims in published maps and institutional affiliations.